ACS APPLIED MATERIALS & INTERFACES

RESEARCH ARTICLE

www.acsami.org

Functionalizing Metal Nanostructured Film with Graphene Oxide for Ultrasensitive Detection of Aromatic Molecules by Surface-Enhanced Raman Spectroscopy

Xiaojuan Liu,[†,‡] Linyuan Cao,[†,‡] Wei Song,[†] Kelong Ai,[†] and Lehui Lu*[,†]

[†]State Key Laboratory of Electroanalytical Chemistry, Changchun Institute of Applied Chemistry, Chinese Academy of Sciences, 5625 Renmin Street, Changchun 130022, P. R. China

[‡]Graduate School of the Chinese Academy of Sciences, Beijing 100039, P. R. China

Supporting Information

ABSTRACT:

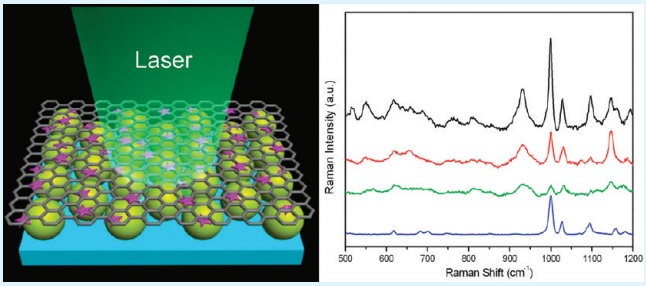

Surface-enhanced Raman spectroscopy (SERS) as a powerful analytical tool has gained extensive attention. Despite of many efforts in the design of SERS substrates, it remains a grand challenge for creating a general substrate that can detect diverse target analytes. Herein, we report our attempt to address this issue by constructing a novel metal-graphene oxide nanostructured film as SERS substrate. Taking advantages of the high affinity of graphene oxide (GO) toward aromatic molecules and the SERS property of nanostructured metal, this structure exhibits great potential for diverse aromatic molecules sensing, which is demonstrated by using crystal violet (CV) with positive charge, amaranth with negative charge, and neutral phosphorus triphenyl (PPh_3) as model molecules.

KEYWORDS: graphene oxide, nanostructures, self-assembly, sensors, surface-enhanced Raman spectroscopy

1. INTRODUCTION

Surface-enhanced Raman spectroscopy (SERS) as a powerful analytical technique for ultrasensitive chemical[1−5] or biochemical[6,7] analysis has gained much attention since its discovery 30 years ago, because it can produce several orders of magnitude enhancement in Raman signals. It has been generally accepted that the large enhancement of normally weak Raman signals arises from an electromagnetic (EM) mechanism and a chemical (charge transfer or CT) mechanism.[8] Electromagnetic mechanism is based on the enhancement of the local electromagnetic field, while chemical mechanism is based on charge transfer between adsorbed molecules and metal surface.[8] The SERS effect is dominated by the strong electromagnetic field enhancement near metallic nanostructures, which is due to the excitation of the localized surface plasmon resonance (LSPR) on the metal surface.[8] Thus, the analytical applications of SERS technique depend strongly on the LSPR properties of the nanostructured metal. To apply SERS in routine studies for molecular sensing purpose, SERS-active substrate should be reproducible, uniform, inexpensive, and easy to be fabricated. Previous investigations on properties of self-assembled nanosized particles suggested that noble metal nanoparticles (such as Au and Ag NPs) assembled on silane-modified glass holds great potential as a SERS sensing platform.[9]

In addition to the nanostructured metal, the SERS signal intensities of the analytes also rely on the amount of molecules in the enhancement region. However, the adsorption ability of analytes onto the metal surface has a strong relation with their molecular structure and charge, and hence applications of this promising technique for direct analysis of diverse aromatic molecules have been restricted by the poor affinity of some target molecules toward the metal surface. To address this issue, various approaches have been proposed for specific tuning of the experimental conditions for each particular analyte. One of the most commonly used methods is to promote the electrostatic interaction between the analyte and the surface of the noble metal by controlling the pH of the medium[10,11] or the potential of roughened metallic electrodes.[12] Although this approach has been successfully applied in sensing some molecules, which carry

Received: March 18, 2011
Accepted: July 5, 2011
Published: July 05, 2011

charge or undergo ionization in alkaline or acidic solution, it does not fulfill the requirements for SERS sensing of noncharged analyte. Another alternative relies on the modification of the metal surface by different surface functional groups (e.g., calixarenes,[13] viologen dications,[14] cyclodextrin derivatives[15,16]), which cause the polycyclic aromatic compounds to be in close proximity to the surface of the metal. Nevertheless, the fixed internal cavities of the host molecules make them only trap organic molecules whose sizes match with the cavities. Therefore, it is highly desirable to develop a general and sensitive SERS substrate for the detection of diverse aromatic molecules. Fortunately, the recently reported applications of graphene oxide (GO) in biosensing[17−20] and drug delivery,[21,22] based on its high affinity to aromatic molecules, indicated that GO is an ideal host material to adsorb a wide variety of molecular analytes and guided us in our formulation of a solution to this problem.

Graphene oxide (GO), which can be prepared in bulk quantities through oxidative exfoliation of graphite,[23−25] is a chemically modified two-dimensional atomically thick carbon network containing hydroxyl and epoxy functional groups on either side of its basal plane in addition to carbonyl and carboxyl groups located at the sheet edges.[26,27] From the chemical point of view, the presence of oxygen functionalities at GO surface may be very interesting because they can provide reactive sites for chemical modification of the carbon network by grafting atoms or molecules.[28] Furthermore, because of the presence of aromatic domains, the functionalized GO can also undergo noncovalent interactions with π-electron-rich molecules.[19] Those superior properties of GO, especially the large surface area, and the presence of two hydrophobic polyaromatic basal planes offer GO a high adsorption capacity toward aromatic compounds. We believe that proper functionalization of metal surface with GO may serve as a means to trap aromatic molecules and get them sufficiently close to the metal surface for providing strong SERS signals.

The metal−graphene composites have attracted tremendous attention in recent years due to their unique properties. Several investigations have been carried out to synthesize nanohybrid structures of GO with noble metal, especially Au and Ag. Various gold nanostructures, such as AuNPs,[29−32] Au rod,[33] and dendritic "snowflake-shape" Au nanostructures[34,35] have been successfully assembled onto GO sheets by the in situ chemical reduction of gold ions and the ex situ adsorption of AuNPs. The growth of gold nanostructures on a graphene-based substrate has been further investigated by Berry et al[35] and Min et al.[36] Similarly, AgNPs[37,38] and Ag films[39] have been directly synthesized on GO substrates by in situ reduction of silver ions or silver mirror reaction. Moreover, Fu et al. reported the sandwich structure of AgNP−GO−Ag piece, in which 3-mercaptopropyltrimethoxysilane (MPTMS) silylated GO played as a bridge to connect AgNPs with Ag piece.[40] It is well-known that Au and Ag nanoscale features can magnify weak Raman signals of molecules near the metal surface. Consequently, the metal−GO composites are excellent candidates for SERS based sensor and this has been demonstrated by using some molecules with high affinity to noble metal particle (i.e., R6G, ATP) as Raman probe molecules.[29,38,41,42] In addition, Raman spectroscopy has been employed extensively to probe the structural characteristics and properties of graphene derivatives, as well as the charge transfer between graphene and the adsorbed or intercalated molecular species.[43−45] Thus, the reported noble metal−GO hybrids offer the opportunities for SERS to facilitate the study of graphene sheets in detail.[31,33−36,39,40] Nevertheless, in comparison with previous investigations focused on the SERS spectra of graphene derivatives, little attention has been paid to the application of metal−GO composites in chemosensing of small organic molecules by taking advantages of the SERS property of metal nanoparticles and the high affinity of aromatic molecules toward GO. Besides, recent experiments have shown that the mechanically exfoliated graphene[46] and mildly reduced graphene oxide[47] can enhance the Raman signals of adsorbed dyes. Such enhancement is believed to be caused by the easy electron transfer between graphene and the molecules adsorbed on its surface, which belongs to the chemical enhancement mechanism.[46] Although the charge-transfer process itself has not been well understood, such graphene-enhanced Raman scattering will further improve the SERS intensities.

With these in mind, we explored herein the potential of GO as a host material to capture diverse aromatic molecules in proximity of the metal nanoparticles for SERS detection. In our strategy, GO sheets were first reacted with 3-mercaptopropyltrimethoxysilane (MPTMS) to introduce multiple thiol groups onto GO. Then the MPTMS-functionalized graphene oxide (fGO) sheets were grafted onto self-assembled silver nanoparticles (AgNPs) film to engineer a metal-graphene oxide complex structure through the formation of strong Ag−S bond. The resultant complex structure was supposed to possess the combined properties of fGO and nanostructured metal, including the high affinity of fGO toward aromatic molecules and the LSPR-based SERS property of AgNPs. These unique properties facilitated the application of this structure as SERS active substrates for carrying out molecule sensing. To demonstrate this, the performance of such structure as SERS substrates was investigated by using positively charged crystal violet (CV), negatively charged amaranth and neutral phosphorus triphenyl (PPh_3) as model molecules.

2. EXPERIMENTAL SECTION

Materials. All chemical regents and solvents were obtained from commercial suppliers and used without further purification. Silver nitrate, 3-mercaptopropyltrimethoxysilane (3-MPTMS), graphite powers were purchased from Alfa Aesar. Sodium citrate and 3-aminopropyltriethoxysilane (3-APTES) were obtained from Sigma-Aldrich. Deionized water (resistance >18.2 MΩ cm^{-1}) was used in all reactions.

Functionalization of Graphene Oxide (GO). GO was prepared according to a modified Hummers method.[23−25] The obtained GO powder (5 mg) was dispersed in ethanol (40 mL) by sonication. To perform the organic reaction, MPTMS were added to the GO suspension. Subsequently, the mixture was heated to 70 °C and aged at that temperature for 3 h under constant stirring. The entire reaction was conducted in an argon atmosphere to prevent the oxidation of SH. The resulting fGO was centrifuged at 10 000 rpm for 10 min, washed with ethanol three times to remove the excess MPTMS, and redispersed in dimethylformamide (DMF).

Preparation of Colloidal Silver Nanoparticles (AgNPs). Colloidal silver was prepared by an aqueous reduction of silver nitrate with trisodium citrate using a method of Lee and Meisel.[48] In brief, silver nitrate (18 mg) was dissolved in deionized water (100 mL) and rapidly heated to boiling point under vigorous stirring. Then two milliliters of 1% (w/v) solution of trisodium citrate was added to the solution and the solution was held at boiling point for 90 min until continuous stirring upon cooling.

Fabrication of the Metal-Graphene Oxide Nanostructured Film. AgNPs were assembled on glass substrate in the following

procedure: First, a glass substrate was cleaned by sequential ultrasonication in acetone, ethanol, deionized water for 15 min in each and then treated with H_2SO_4/H_2O_2 (3:1 (v/v) H_2SO_4 (98%)/H_2O_2 (30%)) at 80 °C for 30 min to derive a hydroxyl surface. After thorough rinsing with Milli-Q ultrapure water and ethanol, the cleaned glass substrate was dried in air. Second, the clean glass substrate was immersed in a 10% solution of APTES in ethanol for 16 h to make the glass silane modified. The substrate was then rinsed profusely with ethanol to remove unbound monomer from the surface and dried in air. Third, the silane modified glass substrate was submerged into colloidal AgNPs for 6 h, resulting in the formation of a layer of AgNPs on the glass surface. Finally, the glass substrate was modified with the functionalized graphene oxide (fGO) by immersion in a solution of fGO in DMF for 3 h at room temperature.[49] For analyte sensing, the resulted substrate was incubated with analyte solution (1 mL) at room temperature overnight. Subsequently, the substrate was picked out, rinsed with solvent, and dried with an argon stream.

Characterization. Transmission electron microscope (TEM) images were obtained using a TECNAI G2 high-resolution transmission electron microscope. Energy-dispersive X-ray spectra (EDS) were collected on the TECNAI G2 with an EDAX detector. Scanning electron microscope (SEM) images were taken with a FEI/Philips XL30 ESEM FEG field-emission scanning electron microscope. X-ray photoelectron spectroscopy (XPS) measurement was performed on an ESCALAB-MKII 250 photoelectron spectrometer with Al Kα X-ray radiation as the X-ray source for excitation. XRD data were measured on a D/Max 2500 V/PC X-ray diffractometer with a Cu Kα X-ray radiation source. UV−visible absorption spectra were carried out by using a Varian Cary 50 UV−vis spectrometer. Raman spectra were recorded with a Renishaw 2000 equipped by an Ar ion laser giving the excitation line of 514.5 nm and an air-cooling charge-coupled device (CCD) as the detector. The laser beam was focused on a spot with a diameter of approximately 1 μm using 25% laser power (25 mW at 100%). The data acquisition time was 10 s for one accumulation. The Raman band of a silicon wafer at 520 cm^{-1} was used to calibrate the spectrometer.

3. RESULTS AND DISCUSSION

Preparation and Characterization of Functional GO (fGO). Figure 1 illustrates the synthetic strategy for fGO sheets through the covalent interaction between GO and 3-mercaptopropyltrimethoxysilane (MPTMS). MPTMS was adopted to functionalize GO due to the following reasons: First, MPTMS can be bound chemically to GO via hydroxyl and carboxyl groups[49] present on the surface of GO; Second, MPTMS is known to undergo self-polymerization in an ethanol solution. Hence, it is speculated that a number of thiol groups can be further introduced by self-polymerization of MPTMS[49] after it binds to individual hydroxyl groups on the basal planes or carboxyl groups located at the sheet edges of GO. Third, the thiol terminated groups from MPTMS can serve as an important coupling agent between fGO and metal nanoparticles, which allows fGO to be immobilized on the AgNPs film.

The morphology of GO before and after functionalization were investigated by transmission electron microscopy (TEM). TEM image of the GO sheets (Figure 2A) clearly illustrated the flake-like shape with some corrugations, whereas the functionalized sample exhibited more wrinkled and folded sheet structure (Figure 2B). The more wrinkled topology might be caused by the functional groups and the extremely small thickness of the resulting fGO. Furthermore, the energy-dispersive X-ray spectra (EDS) taken on these samples (see Figure S1 in the Supporting Information) revealed that both samples consisted of the

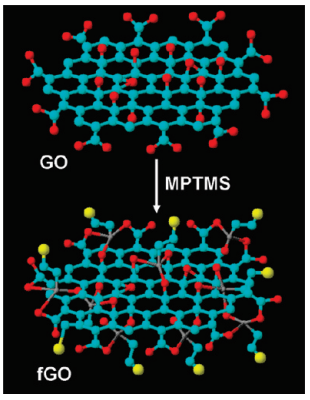

Figure 1. Schematic illustration of the preparation of fGO (cyan, C; red, O; gray, Si; yellow, S).

elements of C, O, S, and Cu. The signals of C and O originated from GO, whereas Cu element resulted from the copper grids. However, the small amount of S element contained in GO was supposed to be induced by H_2SO_4 or $K_2S_2O_8$ employed in the preparation process of GO.[50] Compared with GO, the presence of S element in fGO was anticipated to originate from MPTMS, as stated below. Additionally, the fGO containing Si element, apart from the initial C, O, S, and Cu, which also confirmed the successful functionalization of GO.

To study whether the chemical functionalization would affect the carbon framework of GO sheets or not, the corresponding Raman spectra were collected. As shown in Figure 2C, the Raman spectra of fGO was similar to that of GO, revealing that there was no significant structural change of the carbon framework during the chemical processing from GO to fGO. The well-known D band and G band were clearly observed from both GO and fGO. The D band at 1352 cm^{-1} is a disorder-activated Raman mode that indicates extensive oxidation of the graphite, whereas the G peak centered at 1595 cm^{-1} is characteristic of the sp^2-hybridized carbon atoms in the hexagonal framework,[51,52] which is important for the adsorption of molecules through nonconvalent interaction.

To further verify the presence of the organic groups involved in the reaction, we characterized GO and fGO by X-ray photoelectron spectroscopy (XPS), a direct method for determining the surface element compositions and their chemical environments (Figure 2D). For both survey scans, the observed sharp peaks at 285 and 532 eV corresponded to the characteristic peaks of C1s and O1s, respectively. Moreover, these surveys also showed the presence of S. But the high-resolution scans shown in the inset revealed that the observed binding energy for S was different, suggesting that the S atoms present in GO and fGO were essentially in different electronic environment. The peak at 163.1 eV is assigned to the thiol group originating from MPTMS,[53,54] whereas the broad peak at 168.8 eV is due to the high oxidized S introduced by H_2SO_4 or $K_2S_2O_8$.[55,56] In addition to C, O, and S peaks, the survey of fGO also showed Si peaks, indicating the existence of Si element in the sample. These peaks were entirely absent from the XPS survey scan of GO, which suggested that the covalent functionalization of GO by MPTMS was achieved. Figure 2E, F showed high-resolution narrow scans from the carbon region of GO and fGO, respectively. Three contributions to the C1s core level region recorded for GO can be identified: A first main peak at a binding energy of 284.55 eV

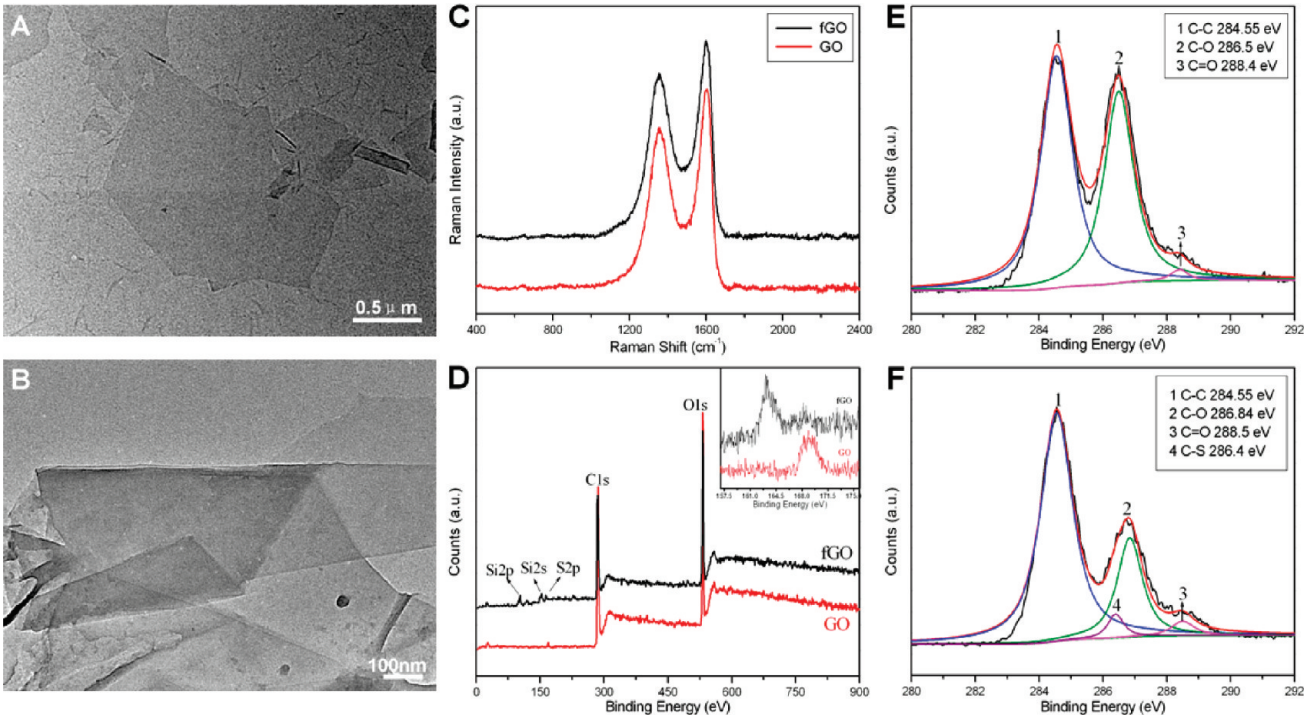

Figure 2. Characterization of synthesized GO and fGO: (A, B) TEM images of GO (A) and fGO (B); (C) Raman spectra of GO and fGO; (D) XPS survey spectra of GO and fGO; inset: the high-resolution curves of the S 2p peaks; (E, F) the deconvolution of C1s spectra of GO (E) and fGO (F).

was attributed to the C−C bonds of GO sheet. A second peak corresponding to carbon bound to oxygen was seen at 286.5 eV, whereas the C═O contribution was found at 288.4 eV. In comparison to GO, the C1s XPS spectrum of fGO contained an additional component peak at 286.4 eV corresponding to the S-bonded carbon atoms,[53] which further validated that MPTMS molecules were effectively decorated on the thin GO sheets. Also, it is observed that the peak intensity ratio between C−C and C−O bond increased, this mainly arises from the overlying of the carbon signal of GO and the grafted MPTMS moieties, which increased the intensity of C−C bond.

Fabrication and Characterization of fGO-Modified AgNP Nanostructured Film. The metal nanoparticle−graphene oxide nanostructured film was fabricated through the following steps. First, glass substrate was modified by silanization with 3-aminopropyltriethoxysilane (APTES), resulting in the formation of an amino-terminated silane monolayer on the glass surface. Next, after being dried in air, the APTES-modified substrate was reacted with colloidal suspension of AgNPs, which led to the production of silver film on the surface of the glass substrate. Finally, fGO sheets were adsorbed on the surface of the self-assembled AgNPs through its thiol group.

The successful assembly of AgNPs onto the glass substrate was illustrated by scanning electron microscopy (SEM). It was evident from Figure 3A, B that the AgNPs attached on the silane-modified glass substrate were homogeneously distributed on the surface. When fGO was grafted onto the surface of AgNPs film, the almost transparent carbon sheets were hard to distinguish due to the extremely small thickness of the fGO sheets, which also suggested their single or few-layer nature. However, the edges and crumpled silk waves of these carbon sheets led us to believe that the fGO was successfully grafted onto the surface of AgNPs film (Figure 3C−E). It should be note that the MPTMS molecules decorated on the GO play a pivotal role in the formation of Ag/fGO composites. When unfunctionalized GO was used under the same experiment conditions, no GO was observed on the surface of the AgNPs film (see Figure S2 in the Supporting Information).

To examine the mono- or few-layer nature of the fGO in the composite system, we scratched part of the AgNPs/fGO film and put it on a copper grid to perform TEM analysis. Although there were some distortions and folds of the fGO film, the mono- or few-layer nature of fGO can still be observed in the TEM image (Figure 3F). The few-layer nature of fGO was further confirmed by the appearance of the 2D band in the Raman spectrum of AgNPs/fGO composite (see Figure S3 in the Supporting Information).[57,58] The AgNPs films with and without fGO modification were further assembled on the silicon wafers and the topography of the films was characterized by atomic force microscopy (AFM). Evident from Figure 3G, the AFM image of the AgNPs film was similar with its SEM images. The corresponding cross-sectional view indicated that the particle height (h_{Ag}) was about 55 nm and the silicon wafer substrate was smooth (Figure 3I). After fGO was anchored on the AgNPs film, the AgNPs can also be visualized in the AFM image (Figure 3H), but the observed height profile of AgNPs (h) was decreased, namely $h < h_{Ag}$, and some small peaks corresponding to corrugated fGO were also detected (indicated by the arrows in Figure 3J). These suggested that fGO has been successfully modified on the AgNPs film. It was noted that the wrinkles of fGO were emanating from silver nanoparticles, and hence the fGO was expected to cover on the AgNPs like a silk veil, as outlined in Figure 3K. Such AgNPs/fGO structure facilitated the fGO as a host material to capture analytes near the surface of the AgNPs as many as possible.

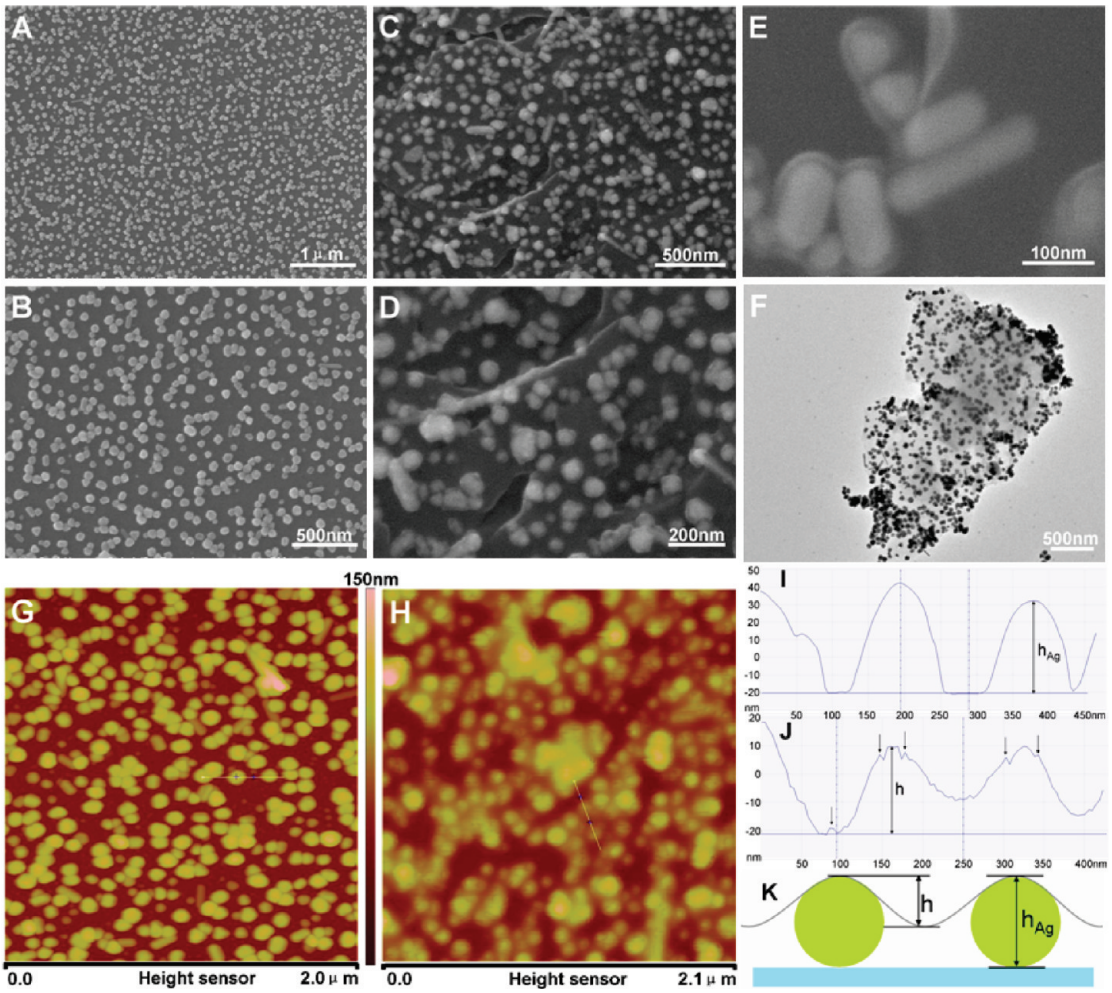

Figure 3. (A−E) Low- and high-magnification SEM images of assembled AgNPs film (A, B) and AgNPs/fGO nanostructured film (C−E). (F) TEM image of the scratched AgNPs/fGO composite. (G, H) The typical AFM images of AgNPs film (G) and AgNPs/fGO nanostructured film (H). (I, J)The cross-section analyses of G and H, respectively. (K) Schematic illustration of the profile of AgNPs/fGO film.

To further corroborate the modification of the AgNPs film on the glass substrate by fGO, XPS was employed to analyze the AgNPs/fGO composites (Figure 4A). The survey scan showed the presence of silver, carbon, oxygen elements, together with silicon element on the sample. The detected silver was attributed to the assembled AgNPs. The silicon mainly originated from fGO and the glass substrate as it cannot be completely covered by the AgNPs. Besides, the high concentration of carbon contained in both the AgNPs film (Figure 4B) and the AgNPs/fGO nanostructured film (Figure 4C) may be due to capping agents of the AgNPs, the APTES located on the exposed areas of the glass substrate, as well as fGO in the AgNPs/fGO nanostructured film. The specific signal of oxygen must be also related with fGO sheets and the capping agents. Furthermore, the high-resolution XPS spectrum of the Ag 3d region shown in the inset consisted of a spin−orbit coupling doublet with binding energy of 368.1 eV for Ag $3d_{5/2}$ state and 374.1 eV for the Ag $3d_{3/2}$ state, which corresponded to the Ag^0 state.[59] Additionally, the C1s XPS spectra of AgNPs film before and after modification by fGO were also collected (Figure 4B, C). In brief, both of the spectra showed four relatively well-resolved peaks corresponding to carbon atoms in different chemical environments. In the absence of fGO, the C−C and C−OH peaks were assigned to the capping agents and APTES. However, after the decoration of fGO, the peak intensity of C−O bond at 286.5 eV increased relative to that of C−C, C−OH, and C═O. This is due to the presence of fGO, which possess higher peak intensity of this component (Figure 2F). The fGO sheets and AgNPs/fGO nanostructured film were also characterized by X-ray diffraction (XRD) (Figure 4D). XRD pattern of fGO revealed an intense, sharp peak centered at $2\Theta = 10.58°$, corresponding to the (001) reflection of GO.[39] In the case of AgNPs/fGO nanostructured film, two peaks were observed at $2\Theta = 38.17°$ and 44.43°, which can be indexed to the (111) and (200) reflections of cubic metal silver, respectively (JCPDS 04−0783). Specially, no obvious diffraction peak attributed to fGO was observed, which indicated that the fGO had almost no aggregation.

SERS Properties and Application. The as-prepared AgNPs/fGO nanostructured film was used as SERS substrate for organic molecule sensing. To investigate the effect of fGO on the SERS performance, we prepared the self-assembled AgNPs film and fGO-modified AgNPs film for comparison. The molecules on the as-prepared two kinds of SERS substrates are schematically shown in pictures A and B in Figure 5, respectively, whereas Figure 5C−E compared the SERS signal intensities of three Raman probes on the two substrates, respectively. In this case,

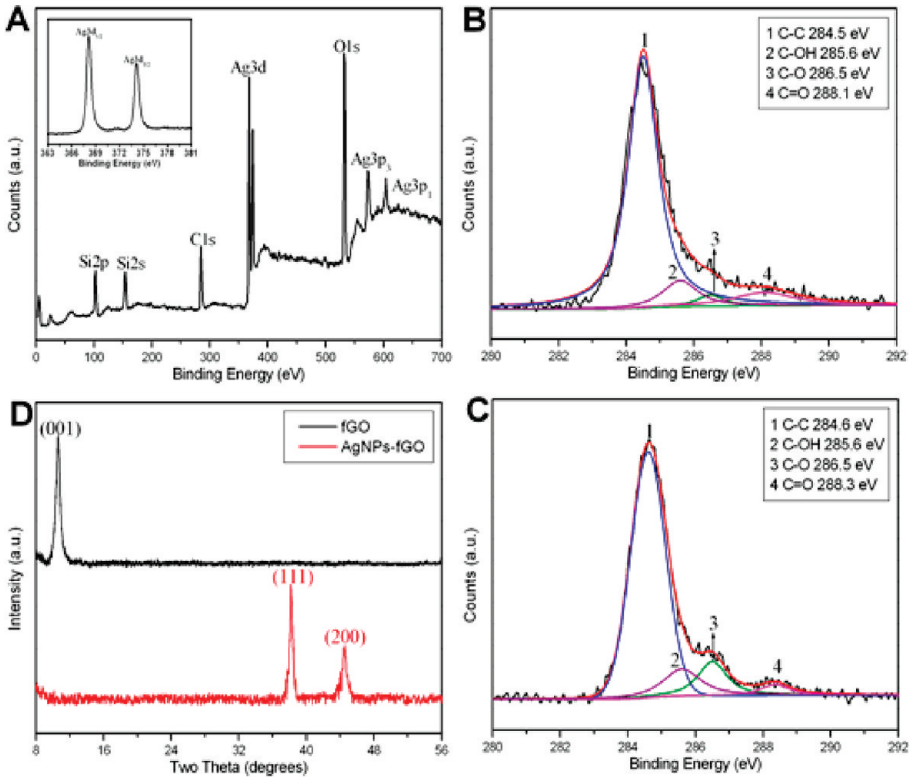

Figure 4. (A) XPS survey spectrum of AgNPs/fGO nanostructured film, inset: high resolution XPS for the Ag 3d signal. (B, C) Deconvoluted high resolution peaks for AgNPs film before (B) and after fGO modification (C). (D) XRD patterns of synthesized fGO and AgNPs/fGO composite.

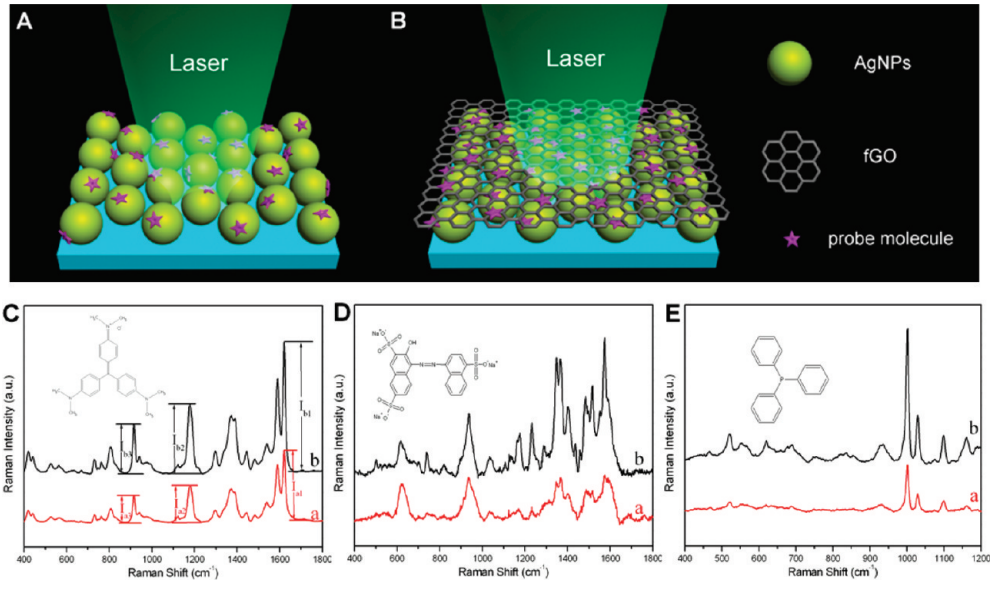

Figure 5. (A, B) Schematic illustrations of the Raman probe molecules on different substrates: self-assembled AgNPs film (A), fGO-modified AgNPs film (B). (C-E) Comparisons of SERS signals of 1×10^{-6} M CV (C), amaranth (D), and PPh_3 (E) on different SERS substrates: a and b correspond to A and B, respectively. Each spectrum is the average of five SERS spectra and has undergone baseline subtraction. The insets show their structures, respectively.

CV (positively charged molecule), amaranth (negatively charged molecule), and PPh_3 (neutral molecule) were used as the model probes. The observed characteristic peaks of these molecules in Figure 5C−E correspond well to the reported Raman spectra of CV,[60] amaranth,[61] and PPh_3,[62,63] respectively. For CV molecule, SERS signals were observed in both cases and the characteristic bands can be clearly distinguished. But the SERS spectra obtained from the fGO-modified AgNPs nanostructured film were more intense. In the cases of amaranth and PPh_3 molecules, the AgNPs film gave only weak enhancements, while

Table 1. SERS Intensity Ratio between the Two Substrates (n) and the Assignments of Several Raman Bands of Three Raman Probe Molecules[a]

probe molecules	Raman Shifts	n	band assignment
CV	1621	1.89	ring C−C stretching
	1179	1.98	ring C−H bending
	915	2.02	ring skeletal vibration
amaranth	1515	3.14	O−H bending + ring stretching
	1402	3.17	C−O stretching +ring stretching
	1231	3.71	C−H bending +C−N stretching
PPh_3	1095	2.76	P−C_{ring} stretching
	1027	2.65	C−H in-plane deformation
	1000	2.88	ring breathing

[a] The assignments of the peaks of CV, amaranth, and PPh_3 are based on previous reports: CV, ref 60; amaranth, ref 61; and PPh_3, refs 62 and 63.

well-resolved spectral peaks were collected on the fGO-modified AgNPs nanostructured film. These observations indicated that fGO modification indeed amplified the SERS signals of the three model molecules. The enhancement effect of fGO modification was quantitative analyzed by applying SERS intensity ratio (n) between the two substrates, described by the following equation: $n = I_{bi}/I_{ai}$. As schematically shown in Figure 5C, I_{ai} and I_{bi} are the intensity of Raman shift i obtained on the AgNPs films before and after the fGO modification, respectively, and do not contain the intensities of baseline. The SERS intensity ratios and the assignments of the Raman bands of the three Raman probe molecules were summarized and compared in Table 1. Obviously, the modification of AgNPs film with fGO had less enhancement effect on CV molecules than that on the other two molecules. This phenomenon can be rationalized by the different affinity of the three molecules on the undecorated AgNPs film. In detail, positively charged CV molecule had strong electrostatic attraction with the negatively charged AgNPs, which enabled the direct adsorption of CV molecules near the metal surface even in the absence of fGO and thus gave high SERS enhancement. In contrast, negatively charged amaranth and neutral PPh_3 molecules had low affinity toward the AgNPs, especially for amaranth molecule. As a consequence, a few molecules can be trapped on the surface of the undecorated AgNPs film, which leaded to low SERS signals of these molecules on AgNPs film alone. However, after the modification with fGO, a large amount of molecules can be adsorbed onto the surface of fGO because of the favorable interactions between them. As a consequence of the proximity of fGO to AgNPs, increased molecules could be trapped in the enhancement region and resulted in better enhanced SERS signals than AgNPs alone.

Nevertheless, if a substrate had poor uniformity and reproducibility, the Raman intensity difference of 2−3 times in SERS measurements would be observed from one spot to another. In order to exclude such influence, we tested the uniformity and reproducibility of the AgNPs film as SERS substrates. Raman spectra of 4-aminothiophenol (4-ATP) molecules at 50 randomly selected spots from five substrates were collected. In the following, we evaluated the reproducibility of the substrate by a new method developed by our group.[64] The resultant SERS-RSD (relative standard deviation) spectra (see Figure S4 in the Supporting Information) showed good reproducibility with the maximal RSD value of the SERS intensities below 15%, which indicated the uniformity and reliability of the AgNPs film as SERS substrates. Such uniformity and reliability further clarified that the increased SERS signals were induced by the modification of AgNPs with fGO. Additionally, we estimated the enhancement ability of AgNPs film quantitatively by calculating the enhancement factor (EF) of 4-ATP molecule adsorbed on the substrate (1×10^{-5} M, 10 μL). The EF was defined as[65]

$$EF = I_{SERS}N_{bulk}/I_{Raman}N_{surface}$$

where I_{SERS} and I_{Raman} stand for the intensities of the same vibrational mode in the SERS and normal Raman spectra, respectively. Both of these data can be directly obtained from the experiment. N_{bulk} and $N_{surface}$ are the number of 4-ATP molecules illuminated by the laser focus spot under normal Raman and SERS condition, respectively. They were calculated on the basis of the estimation of the concentration of the surface species or bulk sample and the corresponding sampling area. Suppose the molecules uniformly dispersed on the film and then the density of the molecules on the film was assumed to be 1×10^{-5} M $\times$ 10 μL $\times$ N_A/cm^2 (the surface area of the substrate is 1×1 cm^2), namely, 6.0×10^{13} molecules/cm^2.[65,66] The laser spot has a 1 μm diameter and the surface area is about 7.9×10^{-9} cm^{-2}, so $N_{surface}$ had a value of 4.7×10^5. Taking the laser spot (1 μm in diameter), the penetration depth (about 2 μm),[65] the molecular weight of 4-ATP (125.19 g/mol) and the density of the solid 4-ATP (1.18 g/cm^3) into account, N_{bulk} had a value of 8.9×10^9 in the detected solid sample area. The intensity of the vibrational mode (ν_{cc}) at 1580 cm^{-1} was used to calculate the EF value. All spectra were normalized for acquisition time and laser power. The EF was calculated to be 1.1×10^5 for the AgNPs film.

On the basis of the above results, the possible effect of fGO on the SERS intensities of the model molecules are considered as follows. First, fGO is a double-sided polyaromatic scaffold with an ultrahigh specific surface area and therefore is capable of adsorbing aromatic compounds. That is, the fGO on the surface of the AgNPs tends to increase the total number of probe molecules on the metal surface, thus resulting in an increase of SERS signals. Second, fGO may chemically enhance the Raman signals of adsorbed molecules, because graphene has been recently reported to be used as substrates for Raman enhancement experiments, and the observed SERS phenomenon has been contributed to chemical enhancement.[46] Accordingly, it is desirable to verify if fGO modification can also induce chemical enhancement in our case. In an attempt to validate this issue, we performed control experiments, in which organic molecules were spin-coated onto the glass surface with and without fGO (see Figure S5A,B in the Supporting Information). In Comparison with the Raman signals from those molecules on the glass substrates, the intensities of CV and amaranth on fGO slightly increased, which revealed that the presence of fGO had chemical enhancement effect. Nevertheless, it was evident that the degree of chemical enhancement was less than that induced by grafting fGO onto AgNPs film in this case. Thus, we speculate that the synergistic effects of increased molecules near the metal surface and fGO-induced chemical enhancement endow the fGO-modified AgNPs nanostructured film with better SERS performances, which further implies that this substrate may be a potential candidate for novel trace analysis of various organic molecules without influence from the charge of analytes.

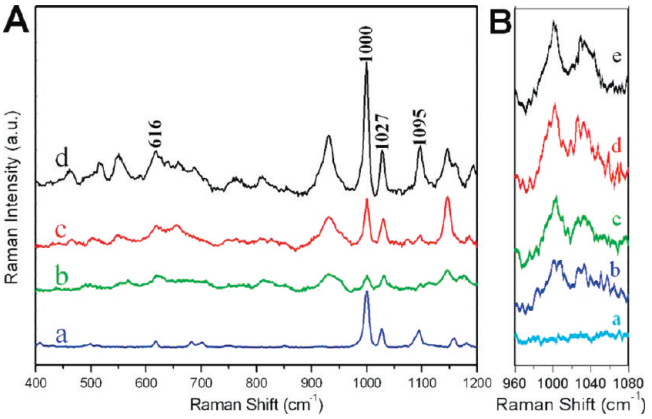

Figure 6. (A) SERS spectra of PPh_3 with different concentrations on the SERS substrates: (a) Raman spectrum of PPh_3 power, (b) 5×10^{-8} M, (c) 5×10^{-7} M, (d) 5×10^{-6} M. Each spectrum has undergone baseline subtraction. (B) SERS spectra of trace level PPh_3 on the SERS substrates in the window of the strongest vibrational band: (a) no PPh_3, (b)1×10^{-9} M, (c) 5×10^{-9} M, (d) 1×10^{-8} M, (e) 1×10^{-7} M.

To prove the affinity of fGO to the analytes, we mixed the solution of fGO with CV, amaranth, and PPh_3 for 12 h, respectively. Any unbound compound was removed by centrifugation. The resulting products were examined by UV−vis spectroscopy. As shown in Figure S6A in the Supporting Information, the fGO dispersion displayed a broad peak near 245 nm, while the free CV solution showed its absorption peaks at 249, 304, and 590 nm. The stacking of CV onto fGO was evident from the spectrum of fGO/CV hybrid solution, which showed the characteristic absorption peaks of CV clearly. Furthermore, as compared to free CV solution, the absorption in the whole spectral region increased without any change in the shape and position. The situation was similar for amaranth and PPh_3 (see Figure S6 B,C in the Supporting Information). These results indicated that fGO had high affinity to these aromatic molecules, which enabled them easily to be adsorbed onto the fGO-modified nanostructured film and thus led to high SERS intensities.

The observed large enhancement and the high affinity of fGO to aromatic molecules suggested that the fGO-modified AgNPs monolayer can indeed serve as robust solid substrates for carrying out molecular sensing with high sensitivity. To demonstrate that they can be readily used for detecting low concentrations of molecules, we selected PPh_3 as the target molecule. Recently, organic phosphorus compounds have attracted much interest because of the extensive applications of the organophosphorus derivatives. For example, they can be used as plasticizers for synthetics, as extraction agents, as oxidation inhibitors for lubricants, as flotation agents, as complexing agents for transition metals, and as insecticides.[67] In addition, several chromogenic and fluorogenic sensors and reagents have been reported for the detection of organic phosphorus compounds with detection limit between 1×10^{-8} M and 5.0×10^{-7} M.[68] Among those organic phosphorus compounds, PPh_3, which has significant detrimental effects on the environment and human health, is one of the most commonly used organophosphorus compounds in the synthesis of organic and organometallic compounds. As a result, it is important to develop highly sensitive, cost-effective sensors that can provide real-time determination of such compounds in the environment. Figure 6A shows the normal Raman (curve a) and SERS spectra (curve b−d) of PPh_3. As compared to the Raman spectra of PPh_3, the characteristic peaks in the present SERS spectra, i.e., 616, 1000, 1027, and 1095 cm^{-1}, could be suggested as the fingerprint vibrational patterns of the PPh_3 trapped by the SERS substrate. These observed Raman and SERS peaks could be assigned based on the previous reports.[62,63] Evidently, SERS intensity of vibrational band at 1000 cm^{-1} is quite sensitive to the concentration of PPh_3. Therefore, such mode was utilized to detect the presence of phosphorus triphenyl compounds in a wide range of concentration from 5×10^{-6} M down to 1×10^{-9} M. When the concentration of the PPh_3 molecules was decreased to 1 nM (Figure 6B), the intensity of the SERS signals became obviously weak, but such mode was still discernible. It is worth noting that the signal-to-noise ratio was larger than 3. Thus, the present detection limit can be as low as 1 nM.

4. CONCLUSIONS

In summary, MPTMS-functionalized GO was successfully grafted onto the surface of the self-assembled AgNPs. Such metal−graphene oxide nanostructured film was an excellent candidate for SERS-based ultrasensitive molecular sensing. It was noteworthy that fGO used in this case not only tended to promote the adsorption of analytes onto the surface of AgNPs, but also provided a chemical enhancement, thus resulting in a considerable increase of Raman signals. Results suggested that it is capable of sensitively detecting a variety of organic molecules, especially aromatic compounds with high affinity toward fGO. Thus, this new family of sensors provides new opportunities for chemical and biological sensing applications.

■ ASSOCIATED CONTENT

Supporting Information. EDS images of GO and fGO; SEM images of assembled AgNPs monolayer immersed in a solution of GO that was not functionalized with MPTMS; Raman background spectra of AgNPs monolayer and Ag/fGO composite; SERS spectra of 4-ATP molecules collected on the randomly selected 50 places from five substrates and the corresponding RSD values curve; Raman spectra of CV and amaranth on glass substrates with and without fGO sheets; UV−vis extinction spectra of three model molecules, fGO, and their complex. This material is available free of charge via the Internet at http://pubs.acs.org/.

■ AUTHOR INFORMATION

Corresponding Author

*Fax: (+86) 431-85262406. Tel: (+86) 431-85262418. E-mail: lehuilu@ciac.jl.cn.

■ ACKNOWLEDGMENT

Financial support by the National Basic Research Program of China (973 Program; 2010CB933600), NSFC (20873138), and the "Hundred Talents Project" of Chinese Academy of Sciences is gratefully acknowledged.

■ REFERENCES

(1) Nie, S.; Emory, S. R. *Science* **1997**, *275*, 1102–1106.
(2) Kneipp, K.; Wang, Y.; Kneipp, H.; Perelman, L. T.; Itzkan, I. R.; Dasari, R.; Feld, M. S. *Phys. Rev. Lett.* **1997**, *78*, 1667–1670.

(3) Li, J. F.; Huang, Y. F.; Ding, Y.; Yang, Z. L.; Li, S. B.; Zhou, X. S.; Fan, F. R.; Zhang, W.; Zhou, Z. Y.; Wu, D. Y.; Ren, B.; Wang, Z. L.; Tian, Z. Q. *Nature* **2010**, *464*, 392–395.
(4) Puebla, R. A.; Cáceres, R. C.; Santos, I. P.; Juste, J. P.; Liz-Marzán, L. M. *Angew. Chem., Int. Ed.* **2008**, *48*, 138–143.
(5) Casadio, F.; Leona, M.; Lombardi, J. R.; Van Duyne, R. *Acc. Chem. Res.* **2010**, *43*, 782–791.
(6) Qian, X.; Peng, X. H.; Ansari, D. O.; Goen, Q. Y.; Chen, G. Z.; Shin, D. M.; Yang, L.; Young, A. N.; Wang, M. D.; Nie, S. *Nat. Biotechnol.* **2008**, *26*, 83–90.
(7) Lu, L. H.; Kobayashi, A.; Tawa, K.; Ozaki, Y. *Chem. Mater.* **2006**, *18*, 4894–4901.
(8) Kneipp, K.; Kneipp, H.; Itzkan, I.; Dasari, R. R.; Feld, M. S. *J. Phys.: Condens. Matter* **2002**, *14*, R597–R624.
(9) Freeman, R. G.; Grabar, K. C.; Allison, K. J.; Bright, R. M.; Davis, J. A.; Guthrie, A. P.; Hommer, M. B.; Jackson, M. A.; Smith, P. C.; Walter, D. G.; Natan, M. J. *Science* **1995**, *267*, 1629–1632.
(10) Billinghurst, B. E.; Oladepo, S. A.; Loppnow, G. R. *J. Phys. Chem. B* **2009**, *113*, 7392–7397.
(11) Qian, X.; Li, J.; Nie, S. *J. Am. Chem. Soc.* **2009**, *131*, 7540–7541.
(12) Li, D.; Li, D. W.; Fossey, J. S.; Long, Y. T. *Anal. Chem.* **2010**, *82*, 9299–9305.
(13) Guerrini, L.; Ramos, J. V.; Domingo, G. C.; Cortes, S. S. *Anal. Chem.* **2009**, *81*, 953–960.
(14) Guerrini, L.; Ramos, J. V.; Domingo, G. C.; Cortes, S. S. *Anal. Chem.* **2009**, *81*, 1418–1425.
(15) Strickland, A. D.; Batt, C. A. *Anal. Chem.* **2009**, *81*, 2895–2903.
(16) Xie, Y.; Wang, X.; Han, X.; Xue, X.; Ji, W.; Qi, Z.; Liu, J.; Zhao, B.; Ozaki, Y. *Analyst* **2010**, *135*, 1389–1394.
(17) Lu, C. H.; Yang, H. H.; Zhu, C. L.; Chen, X.; Chen, G. N. *Angew. Chem., Int. Ed.* **2009**, *48*, 4785–4787.
(18) Jang, H.; Kim, Y. K.; Kwon, H. M.; Yeo, W. S.; Kim, D. E.; Min, D. H. *Angew. Chem., Int. Ed.* **2010**, *49*, 5703–5707.
(19) Balapanuru, J.; Yang, J. X.; Xiao, S.; Bao, Q.; Jahan, M.; Polavarapu, L.; Wei, J.; Xu, Q. H.; Loh, K. P. *Angew. Chem., Int. Ed.* **2010**, *49*, 6549–6553.
(20) Jung, J. H.; Cheon, D. S.; Liu, F.; Lee, K. B.; Seo, T. S. *Angew. Chem., Int. Ed.* **2010**, *49*, 5708–5711.
(21) Liu, Z.; Robinson, J. T.; Sun, X.; Dai, H. *J. Am. Chem. Soc.* **2008**, *130*, 10876–10877.
(22) Zhang, L.; Xia, J.; Zhao, Q.; Liu, L.; Zhang, Z. *Small* **2010**, *6*, 537–544.
(23) Hummers, W. S.; Offeman, R. E. *J. Am. Chem. Soc.* **1958**, *80*, 1339.
(24) Kovtyukhova, N. I.; Ollivier, P. J.; Martin, B. R.; Mallouk, T. E.; Chizhik, S. A.; Buzaneva, E. V.; Gorchinskiy, A. D. *Chem. Mater.* **1999**, *11*, 771–778.
(25) Xu, Y.; Bai, H.; Lu, G.; Li, C.; Shi, G. *J. Am. Chem. Soc.* **2008**, *130*, 5856–5857.
(26) Lerf, A.; He, H.; Forster, M.; Klinowski, J. *J. Phys. Chem. B* **1998**, *102*, 4477–4482.
(27) Dikin, D. A.; Stankovich, S.; Zimney, E. J.; Piner, R. D.; Dommett, G. H. B.; Evmenenko, G.; Nguyen, S. T.; Ruoff, R. S. *Nature* **2007**, *448*, 457–460.
(28) Guo, Y. J.; Guo, S. J.; Ren, J. T.; Zhai, Y. M.; Dong, S. J.; Wang, E. K. *ACS Nano* **2010**, *4*, 4001–4010.
(29) Goncalves, G.; Marques, P. A. A. P.; Granadeiro, C. M.; Nogueira, H. I. S.; Singh, M. K.; Grácio, J. *Chem. Mater.* **2009**, *21*, 4796–4802.
(30) Liu, J.; Fu, s.; Yuan, B.; Li, Y.; Deng, Z. *J. Am. Chem. Soc.* **2010**, *132*, 7279–7281.
(31) Fu, X.; Bei, F.; Wang, X.; Brien, S.; Lombardi, J. R. *Nanoscale* **2010**, *2*, 1461–1466.
(32) Xiang, J.; Drzal, L. T. *ACS Appl. Mater. Interfaces* **2011**, *3*, 1325–1332.
(33) Kim, Y. K.; Na, H. K.; Lee, Y. W.; Jang, H.; Han, S. W.; Min, D. H. *Chem. Commun* **2010**, *46*, 3185–3187.
(34) Jasuja, K.; Linn, J.; Melton, S.; Berry, V. *J. Phys. Chem. Lett.* **2010**, *1*, 1853–1860.
(35) Jasuja, K.; Berry, V. *ACS Nano* **2009**, *3*, 2358–2366.
(36) Kim, Y. K.; Na, H. K.; Min, D. H. *Langmuir* **2010**, *26*, 13065–13070.
(37) Pasricha, R.; Gupta, S.; Srivastava, A. K. *Small* **2009**, *5*, 2253–2259.
(38) Zhou, X.; Huang, X.; Qi, X.; Wu, S.; Xue, C.; Boey, F. Y. C.; Yan, Q.; Chen, P.; Zhang, H. *J. Phys. Chem. C* **2009**, *113*, 10842–10846.
(39) Xu, C.; Wang, X. *Small* **2009**, *5*, 2212–2217.
(40) Fu, X.; Bei, F.; Wang, X.; Yang, X.; Lu, L. *J. Raman Spectrosc.* **2010**, *41*, 370–373.
(41) Rout, C. S.; Kumar, A.; Xiong, G.; Irudayaraj, J.; Fisher, T. S. *Appl. Phys. Lett.* **2010**, *97*, 133108–3.
(42) Huang, J.; Zhang, L.; Chen, B.; Ji, N.; Chen, F.; Zhang, Y.; Zhang, Z. *Nanoscale* **2010**, *2*, 2733–2738.
(43) Ferrari, A. C.; Meyer, J. C.; Scardaci, V.; Casiraghi, C.; Lazzeri, M.; Mauri, F.; Piscanec, S.; Jiang, D.; Novoselov, K. S.; Roth, S.; Geim, A. K. *Phys. Rev. Lett.* **2006**, *97*, 187401.
(44) Krauss, B.; Incze, P. N.; Skakalova, V.; Biro, L. P.; Klitzing, K. V.; Smet, J. H. *Nano Lett.* **2010**, *10*, 4544–4548.
(45) Jung, N.; Crowther, A. C.; Kim, N.; Kim, P.; Brus, L. *ACS Nano* **2010**, *4*, 7005–7013.
(46) Ling, X.; Xie, L.; Fang, Y.; Xu, H.; Zhang, H.; Kong, J.; Dresselhaus, M. S.; Zhang, J.; Liu, Z. *Nano Lett.* **2010**, *10*, 553–561.
(47) Yu, X.; Cai, H.; Zhang, W.; Li, X.; Pan, N.; Luo, Y.; Wang, X.; Hou, J. G. *ACS Nano* **2011**, *5*, 952–958.
(48) Lee, P. C.; Meisel, D. *J. Phys. Chem.* **1982**, *86*, 3391–3395.
(49) Guo, L.; Chen, G.; Kim, D. H. *Anal. Chem.* **2010**, *82*, 5147–5153.
(50) Cao, L. Y.; Liu, Y. L.; Zhang, B. H.; Lu, L. H. *ACS Appl. Mater. Interfaces* **2010**, *2*, 2339–2346.
(51) Stankovich, S.; Dikin, D. A.; Piner, R. D.; Kohlhaas, K. A.; Kleinhammes, A.; Jia, Y.; Wu, Y.; Nguyen, S. T.; Ruoff, R. S. *Carbon* **2007**, *45*, 1558–1565.
(52) Dresselhaus, M. S.; Jorio, A.; Hofmann, M.; Dresselhaus, G.; Saito, R. *Nano Lett.* **2010**, *10*, 751–758.
(53) Hu, M.; Noda, S.; Okubo, T.; Yamaguchi, Y.; Komiyama, H. *Appl. Surf. Sci.* **2001**, *181*, 307–316.
(54) Zuo, J.; Torres, E. *Langmuir* **2010**, *26*, 15161–15168.
(55) Richardson, J.; Johnston, J. H. *J. Colloid Interface Sci.* **2007**, *310*, 425–430.
(56) Stankovich, S.; Piner, R. D.; Chen, X.; Wu, N.; Nguyen, S. T.; Ruoff, R. S. *J. Mater. Chem.* **2006**, *16*, 155–158.
(57) Lee, J.; Novoselov, K. S.; Shin, H. S. *ACS Nano* **2011**, *5*, 608–612.
(58) Lee, J.; Shim, S.; Kim, B.; Shin, H. S. *Chem.—Eur. J.* **2011**, *17*, 2381–2387.
(59) Lu, Z.; Cheng, H.; Lo, M.; Chung, C. Y. *Adv. Funct. Mater.* **2007**, *17*, 3885–3896.
(60) Fathima, S. J. H.; Paul, J.; Valiyaveettil, S. *Small* **2010**, *6*, 2443–2447.
(61) Snehalatha, M.; Ravikumar, C.; Sekar, N.; Jayakumar, V. S.; Joe, I. H. *J. Raman Spectrosc.* **2008**, *39*, 928–936.
(62) Zimmermann, F.; Wokaun, A. *Mol. Phys.* **1991**, *73*, 959.
(63) Song, Y.; Butler, I. S.; Shaver, A. *Spectrochim. Acta. Part A* **2002**, *58*, 2581–2587.
(64) Zhang, B. H.; Wang, H. S.; Lu, L. H.; Ai, K. L.; Zhang, G.; Cheng, X. L. *Adv. Funct. Mater.* **2008**, *18*, 2348–2355.
(65) Sun, Y.; Wang, L.; Sun, L.; Guo, C.; Yang, T.; Liu, Z.; Xu, F.; Li, Z. *J. Chem. Phys.* **2008**, *128*, 074704.
(66) Orendorff, C. J.; Gole, A.; Sau, T. K.; Murphy, C. J. *Anal. Chem.* **2005**, *77*, 3261–3266.
(67) Osman, F. H.; Samahy, F. A. E. *Chem. Rev.* **2002**, *102*, 629–677.
(68) Climent, E.; Martı, A.; Royo, S.; Máñez, R.; Marcos, M. D.; Sancenón, F.; Soto, J.; Costero, A. M.; Gil, S.; Parra, M. *Angew. Chem., Int. Ed.* **2010**, *49*, 5945–5948.